ELSEVIER

Ceramics International 30 (2004) 1041–1047

CERAMICS INTERNATIONAL

www.elsevier.com/locate/ceramint

Effect of titania addition on yttria-stabilised tetragonal zirconia ceramics sintered at high temperatures

Xigeng Miao*, Dan Sun, Pui Woon Hoo, Jianli Liu, Yifei Hu, Yanming Chen

School of Materials Engineering, Nanyang Technological University, Nanyang Avenue, Singapore 639798

Received 1 September 2003; received in revised form 25 September 2003; accepted 22 October 2003

Available online 10 March 2004

Abstract

In order to combine the mechanical properties of yttria-stabilised zirconia (ZrO_2–3 mol% Y_2O_3; code Y–ZrO_2) with the bioactivity of titania (TiO_2), Y–ZrO_2–TiO_2 green compacts with 0–40 vol.% TiO_2 were sintered at 1300, 1400, and 1500 °C for 4 h, respectively. The microstructural features such as grains, pores, and phases were examined using scanning electron microscopy (SEM), X-ray diffraction (XRD), and energy dispersive spectroscopy (EDX). The mechanical properties such as hardness and toughness were also determined using the methods of Vickers indentation and Knoop indentation. All the composites showed the major tetragonal Y–ZrO_2 phase regardless of the content of the added TiO_2. However, rutile TiO_2 phase was obtained at 1300 °C, whereas zirconium titanate ($ZrTiO_4$) phase was found at 1400 and 1500 °C. The Y–ZrO_2–$ZrTiO_4$ composites sintered at 1500 °C showed relatively high hardness (860–1000 kg/mm^2) and toughness (4.0–4.5 MPa m$^{0.5}$), whereas the Y–ZrO_2–TiO_2 composites sintered at 1300 °C had slightly lower hardness (720–950 kg/mm^2) and fracture toughness (3.1–3.3 MPa m$^{0.5}$).

Keywords: A. Sintering; B. Composites; D. TiO_2; D. ZrO_2

1. Introduction

Titania (TiO_2) is a ceramic material, which is generally used as a white pigment or catalyst in manufacturing industries [1,2]. Fine TiO_2 particles with a narrow size distribution are desirable for producing advanced ceramics with enhanced reliability [3]. In recent years, TiO_2 fine particles have become a topic of extensive biological and physico-chemical investigations. TiO_2 surface layers have been coated on metal substrates for extraordinary biocompatibility [4]. The titania coating prepared by a sol–gel technology has recently shown promising bioactivity; titania has the ability to form chemical bonding with living bone in the body [5]. Although titania is inferior to hydroxyapatite in terms of bone apposition rate and bone bonding strength, titania is relatively stable in a biological environment and is able to provide long-term bone bonding [6]. Despite its poor mechanical properties, TiO_2 ceramics are promising for implant applications.

Pure zirconia has three polymorphs: monoclinic, tetragonal, and cubic phases. Due to the large volume change associated with the tetragonal to monoclinic phase transformation, pure zirconia has no practical applications for engineering components. Zirconia can be stabilised with various additives, among which yttria and cerium are the most useful stabilisers. In particular, yttria-stabilised zirconia (ZrO_2), is known to be both hard and tough at room temperature [7]. It also possesses a notably high corrosion resistance in biological environments. However, physico-chemical investigations have proved that although yttria-stabilised ZrO_2 is biocompatible in a biological environment, it cannot form chemical bonding with the surrounding living tissues and hence can only be used as a bioinert material [7,8].

Pure titania is subject to anatase to rutile phase transformation, although the transformation temperature varies. It was reported that the anatase to rutile phase transformation could be retarded by a small amount of zirconia, which was present in the form of solid solution with the host titania [9]. With zirconia as the dopant, anatase phase with high crystallinity and high phase stability was maintained even after annealing at 1000 °C for 1 h [10]. Recent study indicated that the anatase phase was responsible for the formation

* Corresponding author. Tel.: +65-6790-4260; fax: +65-6790-9081.
E-mail address: asxgmiao@ntu.edu.sg (X. Miao).

0272-8842/$30.00
doi:10.1016/j.ceramint.2003.10.025

of the apatite layer [11]. However, the addition of zirconia to titania tends to result in the formation of zirconium titanate, depending on the mixing homogeneity and the sintering temperature. Prepared by a co-precipitation method, a mixed powder with 1 ZrO_2 to 1 TiO_2 molar ratio was amorphous at low temperatures but crystallised into $ZrTiO_4$ at about 700 °C [12,13]. In contrast, conventionally mixed zirconia and titania yielded zirconium titanate $ZrTiO_4$ phase after calcination at 1200–1600 °C [14].

The usefulness and limitations of the zirconia and titania lead to the investigation of ZrO_2–TiO_2 composites in order to achieve both mechanical strength and biological performance. However, sintering of yttria-stabilised zirconia ceramics requires a high temperature, which unfortunately excludes the retention of anatase phase and leads to the formation of zirconium titanate. On the other hand, if anatase phase is to be maintained, the zirconia component cannot be fully sintered, which will eliminate the advantages of the strong and tough zirconia phase. Thus, it seems that a core-layer structured material is needed, wherein the core is made of Y–ZrO_2–$ZrTiO_4$ via a high temperature process whereas the layer as the coating of the core is made of TiO_2–ZrO_2 via a low temperature process. The materials of a strong core-bioactive layer are expected to be useful for dental root implants, which require both mechanical strength and surface bioactivity. This paper presents the work done for the core material and focuses on the microstructural and mechanical characterisation of various compositions of the Y–ZrO_2–TiO_2 composites sintered at different high temperatures.

2. Experimental procedure

Titania (TiO_2) sol was produced from titanium butoxide ($Ti(OC_4H_9)_4$) liquid (Aldrich Chemical Company, Inc.) in the ambient atmosphere. The precursor $Ti(OC_4H_9)_4$ (73.97 g) was first mixed with an excess amount of absolute ethanol (160.4 g) in order to slow down the hydrolysis rate. Then an excess amount of distilled water was added dropwise into the solution that was being stirred at 540 rpm. After 2 h of mixing, the resultant slurry was washed four times using distilled water to remove the excess ethanol. Then a small portion of the TiO_2 sol was dried and calcinated at 600 °C for 1 h. The concentration of the sol was then obtained from the weight of dried TiO_2 powder (g) and the weight of parent TiO_2 sol (g). The remaining TiO_2 sol was kept in a container with cover until further usage.

On the other hand, Y–ZrO_2 powder (ZrO_2–3 mol% Y_2O_3), Aldrich Chemical Company, Inc.) with submicron size was used to produce Y–ZrO_2 sol. The Y–ZrO_2 powder was first mixed with a small amount of distilled water, and then the mixture was subjected to 150 rpm wet ball milling for 60 min at room temperature. An excess amount of distilled water was added into the Y–ZrO_2 slurry after the ball milling. The slurry was mixed by using a magnetic stirring bar for a sufficient time to obtain homogeneous Y–ZrO_2 sol. The weight concentration of Y–ZrO_2 sol was then determined using the weight of the dried Y–ZrO_2 powder (g) and the weight of parent Y–ZrO_2 sol (g).

The Y–ZrO_2–TiO_2 sol mixtures with 0, 10, 20, 30, 40 vol.% TiO_2 were obtained by homogeneously mixing the two sols based on their respective weight concentrations. The sol mixtures were then dried, crushed into powders, and compressed into disk-shaped green compacts, followed by sintering at 1300, 1400, and 1500 °C for 4 h to produce different composite samples. The sintered samples were ground and polished for Vickers indentation and Knoop indentation. Some polished samples were thermally etched at 1300 °C for 1 h to reveal grain sizes.

The microstructural characteristics of the sintered composites were studied using a scanning electron microscope (SEM, JEOL JSM-5410) equipped with an energy dispersive spectrum analysis system (EDX). An X-ray diffractometer (XRD, Shimadzu) with the Cu Kα radiation was also used to examine the crystalline phases in the composites. Vickers hardness (*H*) was measured on HSV-20, SHIMADZU microhardness tester using the following equation:

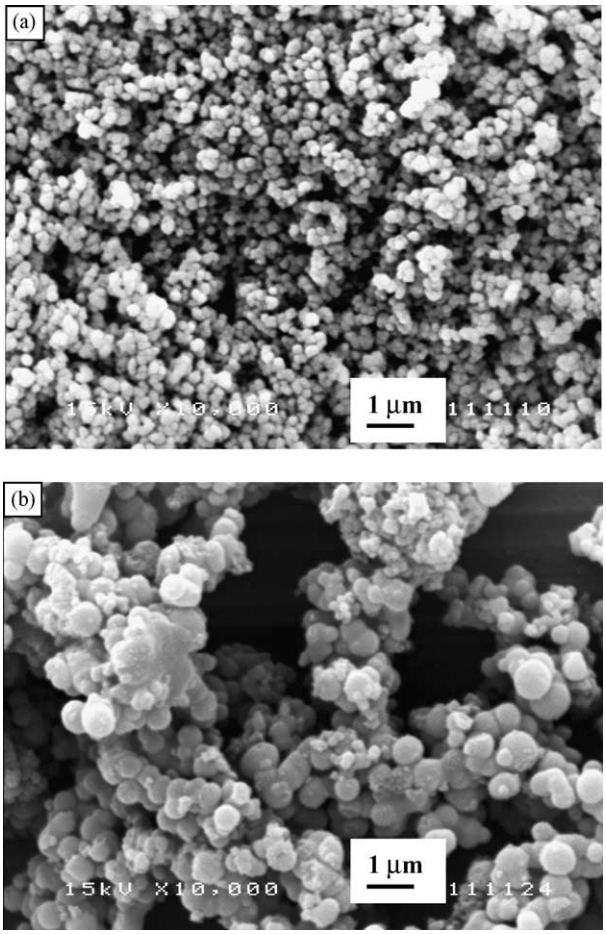

Fig. 1. SEM micrographs of ZrO_2 (3 mol% Y_2O_3) (coded as Y–ZrO_2) powder (a) and TiO_2 powder (b).

$$H = 1.854\frac{P}{d^2} \quad (1)$$

where P is the applied load (kg) and d the average diagonal length of the indentation (mm).

When the Vickers indenter of the microhardness tester was changed to a Knoop indenter, the Young's modulus (E) could be determined using the following equation [15]:

$$\frac{b'}{a'} = \frac{b}{a} - \alpha\frac{E}{H_K} \quad (2)$$

where b'/a' is the indent diagonal ratio after elastic recovery (i.e. after the indentation), b/a is the ratio of the Knoop indenter dimensions (1/7.11), α is a constant with a value of 0.45 and H_K is the Knoop hardness measured. The microhardness tester was also used to measure the fracture toughness (K_{1c}) using the following formula [16]:

$$K_{1c} = 0.016\left(\frac{E}{H}\right)0.5\frac{P}{c^{1.5}} \quad (3)$$

where E is the Young's modulus (GPa), H the Vickers hardness (GPa), P the indentation load (N), c the crack length (m) from the centre of the indentation impression to the crack tip.

3. Results and discussion

3.1. Residual porosity

Fig. 1(a) shows the Y–ZrO_2 particles used in the study. The primary particle size was about 0.3 μm, but the primary particles were grouped into clusters or agglomerates. Fig. 1(b) is the SEM micrograph of the prepared TiO_2 particles used as a starting material in the study. The primary particle size was about 0.6 μm, and again the primary particles formed agglomerates. While the Y–ZrO_2 powder was purchased, the TiO_2 powder was prepared in house. Thus, the process from the precursor of $Ti(OC_4H_9)_4$ to the final TiO_2 particles should be understood. According to Honda et al. [17], the conversion from $Ti(OC_4H_9)_4$ to TiO_2 was based on the following chemical reactions:

$$Ti(OC_4H_9)_4 + 4H_2O \rightarrow Ti(OH)_4 + 4C_4H_9OH$$

(hydrolysis and condensation) (4)

$$Ti(OH)_4 \rightarrow TiO_2 + 2H_2O$$

(calcination at a high temperature) (5)

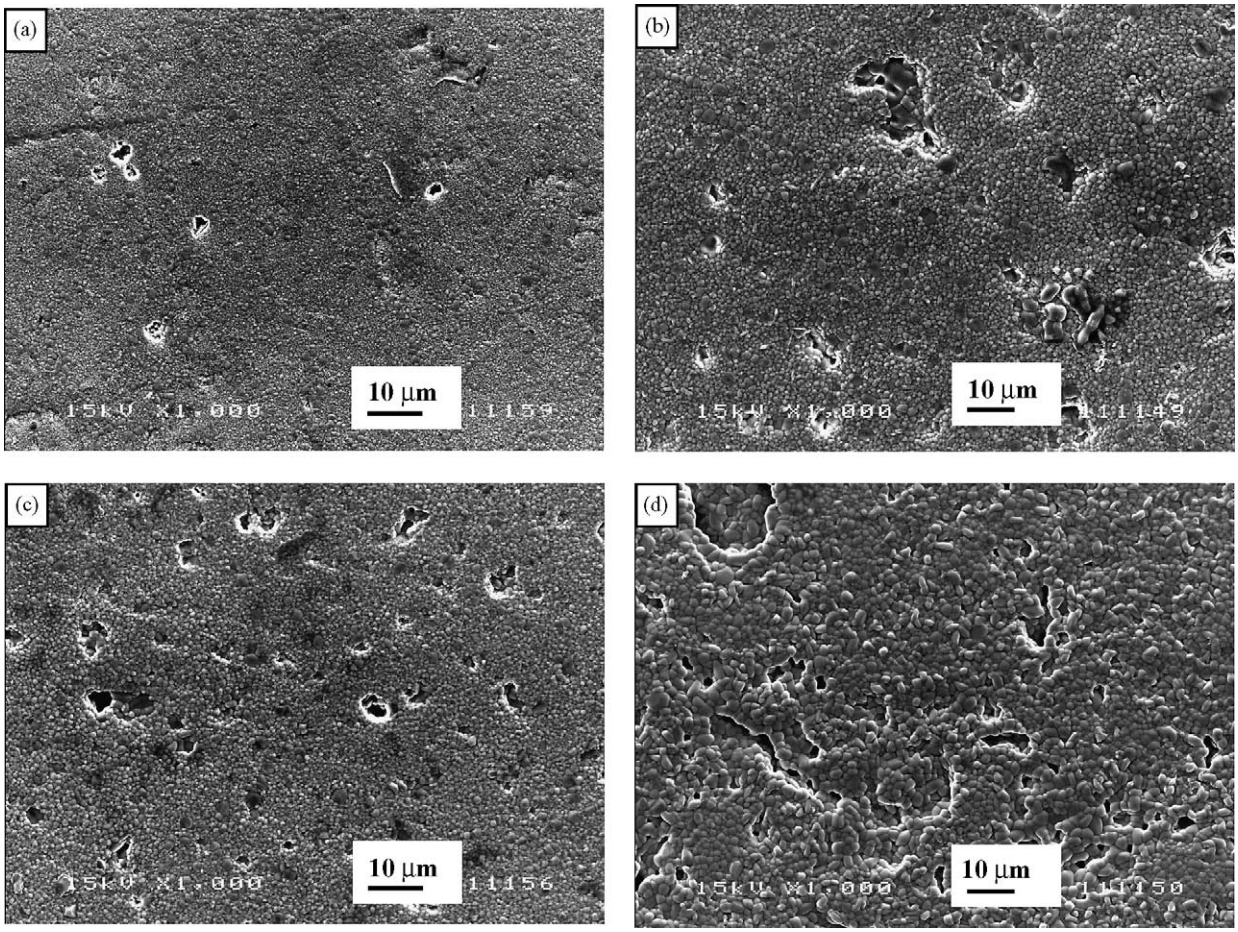

Fig. 2. SEM micrographs of the thermally etched surfaces of the Y–ZrO_2–TiO_2 composites sintered at 1300 °C with TiO_2 content of 0 vol.% (a), 10 vol.% (b), 20 vol.% (c), and 30 vol.% (d).

Since the two kinds of particles were mixed in the state of sols, the homogeneity of mixing was controlled by the particle sizes and also by the sizes of the clusters that were unbroken during the mixing. In current study, the dry pressing method was used, which was simple but had the problem of particle agglomeration. From the wet mixed sols to the dried mixed powders, further agglomeration of particles was expected, due to the nature of the fine particles and the van der Waals forces between them. This agglomeration adversely affected the packing efficiency of the mixed powders and thus affecting the densification and the homogeneity of the sintered Y–ZrO_2–TiO_2 composites.

Fig. 2(a)–(d) show the SEM micrographs of the polished and thermally etched surfaces of the Y–ZrO_2–TiO_2 composites with 0, 10, 20, and 30 vol.% TiO_2, respectively, that were sintered at 1300 °C for 4 h. It appeared that the number of pores (defects) and the size of the pores (defects) increased with the amount of the TiO_2 added into the Y–ZrO_2 powders. It will be seen later that the composites sintered at 1300 °C contained mainly tetragonal zirconia phase and rutile titania phase. Thus, the increased inhomogeneity and porosity with the TiO_2 addition reflected the effect of the severe agglomeration of the TiO_2 particles and the agglomeration between the two mixed powders. The microstructural defects could be minimised by using the well-known colloidal processing methods, which are far more advantageous than the conventional dry pressing in terms of agglomerate removal.

3.2. Densification and $ZrTiO_4$ formation

Fig. 3(a)–(d) show the SEM micrographs of the polished and thermally etched surfaces of the Y–ZrO_2–TiO_2 composites with 0, 10, 20, and 40 vol.% TiO_2, respectively, that were sintered at 1400 °C for 4 h. It appeared that high degree of densification or low residual porosity was achieved for the composites sintered at 1400 °C. The 1500 °C sintering also resulted in higher densification. Apart from the difference in densification between the composites sintered at 1300 °C and those sintered at 1400 and 1500 °C, another significant difference was the formation of compound between the Y–ZrO_2 and TiO_2 when the sintering temperatures were 1400 and 1500 °C.

From Fig. 3(a)–(d), it can be seen that with the addition of the TiO_2, numerous crystals were observed to protrude out of the surfaces. It seemed that the numbers of the crystals

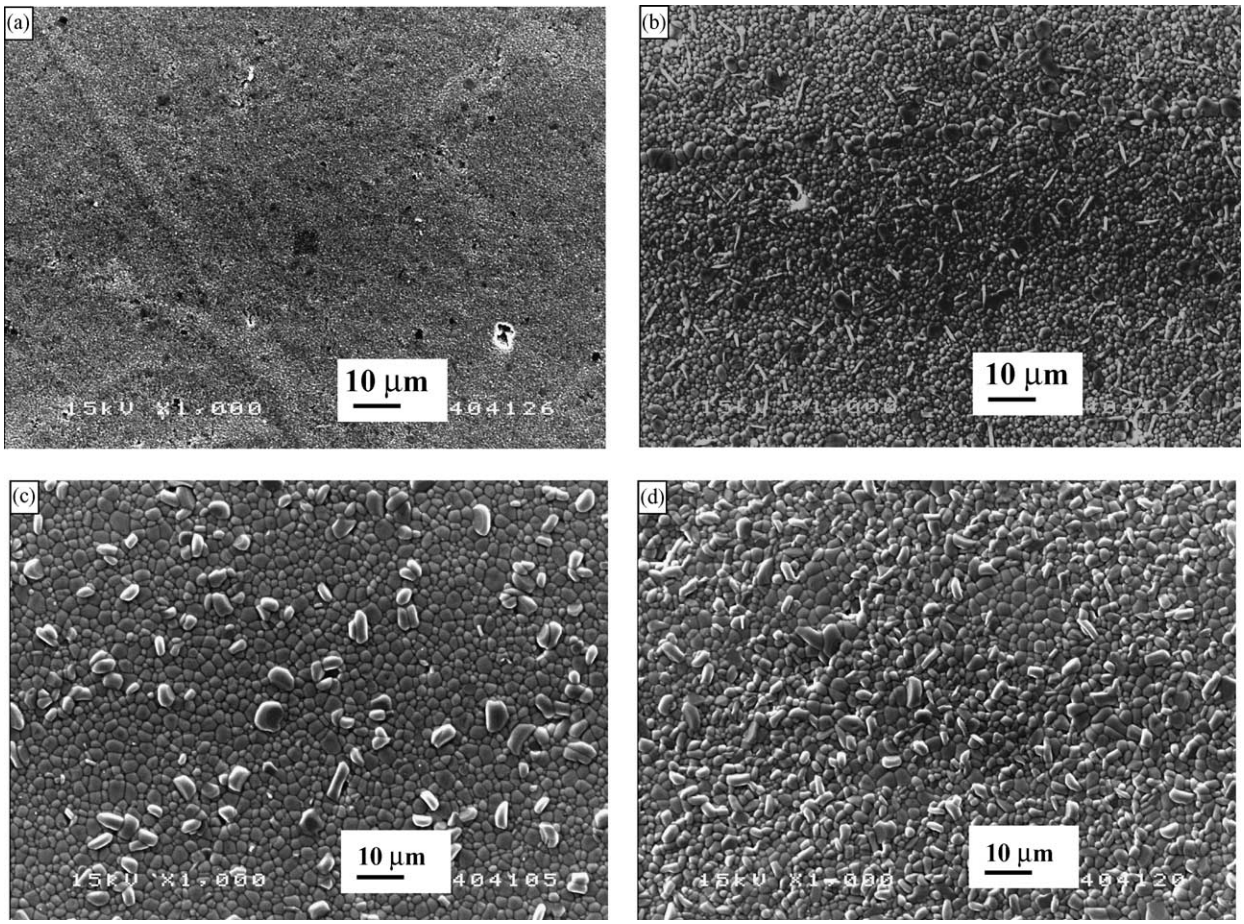

Fig. 3. SEM micrographs of the thermally etched surfaces of the Y–ZrO_2–$ZrTiO_4$ composites sintered at 1400 °C with TiO_2 addition of 0 vol.% (a), 10 vol.% (b), 20 vol.% (c), and 40 vol.% (d).

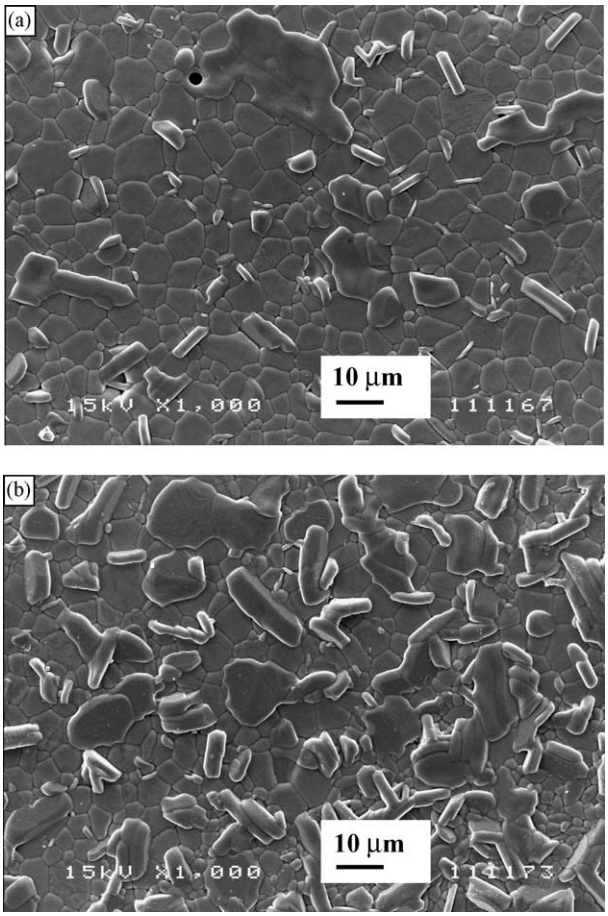

Fig. 4. SEM micrographs of the thermally etched surfaces of the Y–ZrO_2–$ZrTiO_4$ composites sintered at 1500 °C with TiO_2 addition of 20 vol.% (a) and 40 vol.% (b).

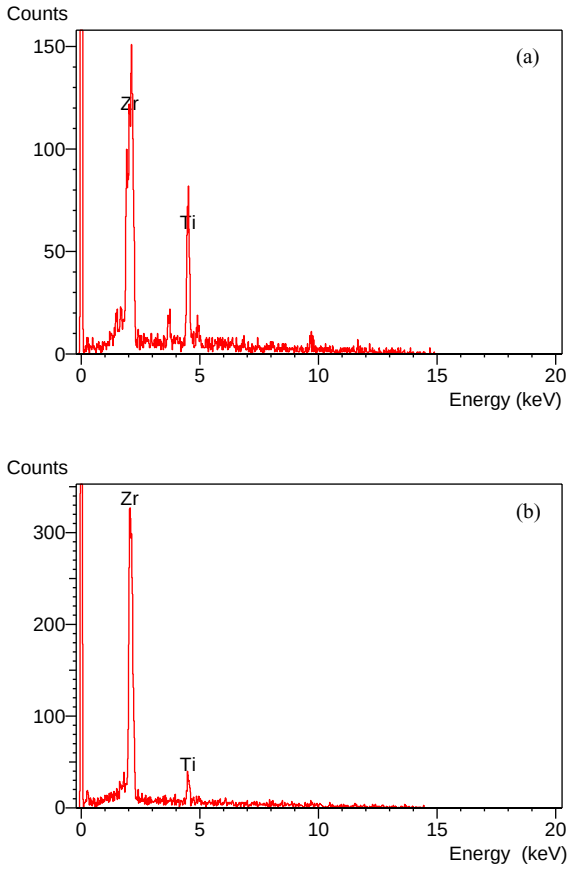

Fig. 5. Energy dispersive spectra from a $ZrTiO_4$ crystal (a) and a Y–ZrO_2 grain (b).

increased with the TiO_2 addition. It will be seen later that the protruding crystals were the $ZrTiO_4$ compound, which was confirmed by the XRD and EDX analyses. The formation of the $ZrTiO_4$ crystals can be more clearly seen from Fig. 4(a) and (b). The content of the compound seemed very high judging from the phase surface area fraction.

3.3. Phase analysis and grain size

The identification of the protruding crystals was done by both EDX and XRD. EDX showed that the protruding crystals contained high Zr and Ti intensities (Fig. 5(a)), whereas the background grains exhibited strong Zr intensity but weak Ti intensity (Fig. 5(b)). Thus, the protruding crystals can be considered as $ZrTiO_4$ phase, whereas the background grains as zirconia phase. However, EDX was not able to determine exclusively the phases present. Thus, XRD was used to analyse the phases. Fig. 6 shows that the XRD patterns of the Y–ZrO_2–40 vol.% TiO_2 composites sintered at 1300 °C (1573 K), 1400 °C (1673 K), and 1500 °C (1773 K). At 1300 °C, only rutile TiO_2 (JCPDS 21-1276) and tetragonal zirconia (JCPDS 17-0923) were observed. At 1400 and 1500 °C, all the TiO_2 reacted with the zirconia to form the $ZrTiO_4$ phase (JCPDS 34-0415). The XRD results for the formation of the $ZrTiO_4$ phase matched well with the SEM micrographs that showed the appearance of the protruding crystals. Detailed examination indicated that there were some shifts of the peak positions for both the zirconia phase and the titania phase. The peak shifts indicated some

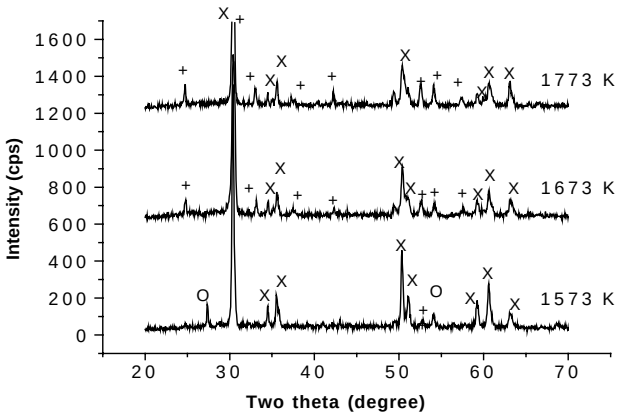

Fig. 6. XRD patterns of the Y–ZrO_2–40 vol.% TiO_2 mixtures sintered at different temperatures; cpc: counts per second; (○): rutile TiO_2 phase; (×): tetragonal Y–ZrO_2 phase; (+): $ZrTiO_4$ phase.

solubilities between TiO_2, ZrO_2, and Y_2O_3 present in the composites.

The variations of the grain size against temperature and composition can be seen from Figs. 2–4. Obviously, the grain size increased with the sintering temperature. More importantly, the grain size also changed with the TiO_2 addition. It was evident that the background grains (mainly Y–ZrO_2) increased in grain size with the addition of TiO_2 until 20 or 30 vol.% TiO_2 addition. However, further addition of TiO_2 led to the decrease of the matrix grain sizes, which could be due to the increased number of the $ZrTiO_4$ crystals that were able to restrict the growth of the matrix grains. The increase of the grain size with TiO_2 addition might be due to the relatively larger titania particles compared to the zirconia particles, due to the fast grain growth rate of the TiO_2 particles, and due to the limited solubility of the TiO_2 in Y–ZrO_2, which enhanced the diffusion rate and thus the grain growth rate.

3.4. Mechanical properties

The hardness of the Y–ZrO_2–TiO_2 composites sintered at 1300 °C is shown in Fig. 7. The hardness obviously decreased with the content of TiO_2. One reason was the low hardness of the titania component in the composites. Another reason was the porosities present in the composites. In general, hardness decreases with porosity. The porosity (P) dependence on the hardness (H) has been studied intensively [18], and one of the many proposed relationships is:

$$H = H_0(1 - P)^2 \exp(-\beta P), \quad \beta < 1 \tag{6}$$

where H_0 is the hardness of dense material counterpart, and β is an empirical factor, without relationship to microstructure. When the empirical factor β is considered as a constant, it can be predicted that hardness decreases with increasing porosity. Therefore the low sintering temperature of 1300 °C, which yielded the relatively high porosities, gave rise to the low hardness values.

The hardness (kg/mm^2) values of the Y–ZrO_2–$ZrTiO_4$ composites sintered at 1500 °C are also shown in Fig. 7. It appeared that the hardness decreased monotonically with the increase of the TiO_2 content. Since TiO_2 reacted with

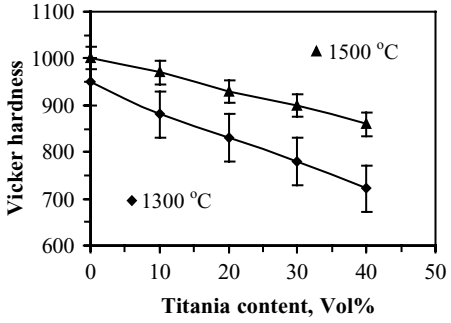

Fig. 7. Vickers hardness (units: kg/mm^2) as a function of titania content for the Y–ZrO_2–40 vol.% TiO_2 mixtures sintered at 1300 and 1500 °C.

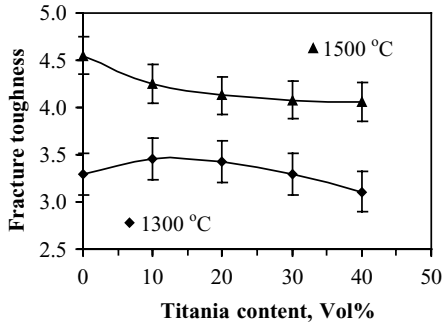

Fig. 8. Fracture toughness (units: MPa m$^{0.5}$) as a function of titania content for the Y–ZrO_2–40 vol.% TiO_2 mixtures sintered at 1300 and 1500 °C.

ZrO_2 to form $ZrTiO_4$ above 1400 °C, the initially batched Y–ZrO_2–TiO_2 composites were actually Y–ZrO_2–$ZrTiO_4$ composites. Thus, the hardness of the composites possibly followed the mixture law:

$$H_c = H_z V_{fz} + H_{zt} V_{fzt} \tag{7}$$

where H_c, H_z, and H_{zt} are the hardness of the composite, the Y–ZrO_2 phase, and the $ZrTiO_4$ phase, respectively, whereas V_{fz} and V_{fzt} are the volume fractions of the Y–ZrO_2 phase and the $ZrTiO_4$ phase, respectively. Since it is difficult to find the data of the mechanical properties of the $ZrTiO_4$ phase from the literature, it can only be said that the hardness of the $ZrTiO_4$ phase should be lower than the yttria-stabilised zirconia (Y–ZrO_2).

Fig. 8 illustrates the fracture toughness (MPa m$^{0.5}$) values of the Y–ZrO_2–$ZrTiO_4$ composites sintered at 1500 °C. The fracture toughness values again decreased with the increasing TiO_2 content. The high toughness of the Y–ZrO_2 ceramics should be related to the transformation toughening mechanism of the Y–ZrO_2 phase. It is well-known that Y–ZrO_2 ceramics have high toughness compared to most other ceramics. According to the transformation toughening mechanism, in the vicinity of a propagating crack, stress-induced transformation from metastable tetragonal ZrO_2 to monoclinic phase will occur [19]. This transformation is accompanied by a volume increase, which generates a compressive stress field around the crack tip, and thus extra energy is required to extend the crack, leading to the high fracture toughness of the ceramics [20]. Therefore, for Y–ZrO_2–$ZrTiO_4$ composites which contained higher Y–ZrO_2 contents, the phase transformation toughening might be more pronounced. However, the decrease of fracture toughness with the TiO_2 addition seemed to slow down after 30 vol.% TiO_2. Thus, additional toughening mechanism related to the $ZrTiO_4$ as a second phase might also be operating in the composites. The second phase obviously created inter-phase boundaries and possibly caused residual thermal stresses in the composites, which might influence the transformation toughening in the composites. As to the fracture toughness values of the Y–ZrO_2–TiO_2 composites sintered at 1300 °C, they should be related to the high porosity level, increased TiO_2 content, and some

grain growth of the zirconia phase, which might affect the transformation toughening mechanism.

4. Conclusions

Ceramic composites of tetragonal Y–ZrO_2 phase and rutile TiO_2 phase with 10, 20, 30, 40 vol.% TiO_2 were prepared by sintering Y–ZrO_2–TiO_2 mixtures at 1300 °C. However, when the mixtures were sintered at 1400 and 1500 °C, the TiO_2 phase disappeared, instead, the $ZrTiO_4$ compound was formed. Thus, Y–ZrO_2–$ZrTiO_4$ composites were formed by means of reaction sintering. The mechanical properties such as hardness and fracture toughness of the Y–ZrO_2–TiO_2 composites and the Y–ZrO_2–$ZrTiO_4$ composites, decreased with the increasing TiO_2 content and decreased with the $ZrTiO_4$ content in the composites. The Y–ZrO_2–$ZrTiO_4$ composites sintered at 1500 °C showed relatively high hardness (860–1000 kg/mm^2) and toughness (4.0–4.5 MPa m$^{0.5}$), whereas the Y–ZrO_2–TiO_2 composites sintered at 1300 °C had slightly lower hardness (720–950 kg/mm^2) and fracture toughness (3.1–3.3 MPa m$^{0.5}$). The Y–ZrO_2–$ZrTiO_4$ composites may have high temperature structural applications, whereas, the Y–ZrO_2–TiO_2 composites can be used for the core material of the dental roots as they still have sufficient mechanical properties compared with currently known bioceramics. The future work would be the study of a bioactive layer on the core material and the investigation of the bioactivity and bone bonding ability of the complex composite system.

Acknowledgements

The authors would like to acknowledge the financial support from the Nanyang Technological University in Singapore (AcRF RG26/01).

References

[1] S. Riyas, V.A. Yasir, P.N.M. Das, Crystal structure transformation of TiO_2 in presence of Fe_2O_3 and NiO in air atmosphere, Bull. Mater. Sci. 25 (4) (2002) 267–273.
[2] R.B. Zhang, L. Gao, Effect of peptization on phase transformation of TiO_2 nanoparticles, Mater. Res. Bull. 36 (2000) 1957–1965.
[3] H.K. Park, D.K. Kim, C.H. Kim, Effect of solvent on titania particle formation and morphology in thermal hydrolysis of $TiCl_4$, J. Am. Ceram. Soc. 80 (3) (1997) 743–749.
[4] V. Faust, F. Heidenau, J. Schmidgal, F. Stenzel, G. Lipps, G. Ziegler, Biofunctional biocompatible titania coatings for implants, Key Eng. Mater. 206–213 (3) (2001) 1547–1550.
[5] P. Li, K. Groot, T. Kokubo, Bioactive hydroxyapatite–titania composite coating prepared by sol–gel process, J. Sol–Gel Sci. Tech. 7 (1/2) (1996) 27–34.
[6] B. Fartash, H. Liao, J. Li, N. Fouda, L. Hermansson, Long-term evaluation of titania-based ceramics compared with commercially pure titanium in vivo, J. Mater. Sci.: Mater. Med. 6 (8) (1995) 451–454.
[7] L. Fu, K.A. Khor, J.P. Lim, Effects of yttria-stabilized zirconia on plasma-sprayed hydroxyapatite/yttria-stabilized zirconia composite coatings, J. Am. Ceram. Soc. 85 (4) (2002) 800–806.
[8] V.J.P. Lima, K.A. Khor, L. Fu, P. Cheang, Hydroxyapatite–zirconia composite coatings via the plasma spraying process, J. Mater. Process. Technol. 89–90 (1999) 491–496.
[9] J. Yang, J.M.F. Ferreira, On the titania phase transition by zirconia additive in a sol–gel-derived powder, Mater. Res. Bull. 33 (3) (1998) 389–394.
[10] M. Hirano, C. Nakahara, K. Ota, M. Inagaki, Direct formation of zirconia-doped titania with stable anatase-type structure by thermal hydrolysis, J. Am. Ceram. Soc. 85 (5) (2002) 1333–1335.
[11] M. Wei, M. Uchida, H.-M. Kim, T. Kokubo, T. Nakamura, Apatite-forming ability of CaO-containing titania, Biomaterials 23 (2002) 167–172.
[12] M. Daturi, A. Cremona, F. Milella, G. Busca, E. Vogna, Characterisation of zirconia–titania powders prepared by coprecipitation, J. Eur. Ceram. Soc. 18 (8) (1998) 1079–1087.
[13] A.K. Bhattacharya, A. Hartridge, K.K. Mallick, D. Taylor, Inorganic sol gel synthesis of zirconium titanate fibres, J. Mater. Sci. 31 (21) (1996) 5583–5586.
[14] G. Colon, M.A. Aviles, J.A. Navio, P.J. Sanchez-Soto, Thermal behaviour of a TiO_2–ZrO_2 microcomposite prepared by chemical coating, J. Therm. Anal. Calorim. 67 (2002) 229–238.
[15] M.A. Camerucci, G. Urretavizcaya, A.L. Cavalieri, Mechanical behaviour of cordierite and cordierite–mullite materials evaluated by indentation techniques, J. Eur. Ceram. Soc. 21 (9) (2001) 1195–1204.
[16] X. Miao, S. Scheppokat, N. Claussen, M.V. Swain, Characterisation of an oxidised layer on reaction bonded mullite/zirconiac by indentation, J. Eur. Ceram. Soc. 18 (6) (1998) 653–659.
[17] H. Honda, K. Suzaki, Y. Sugahara, Control of hydrolysis and condensation reactions of titanium tert-butoxide by chemical modification with catechol, J. Sol–Gel Sci. Tech. 22 (1/2) (2001) 133–138.
[18] J. Luo, R. Stevens, Porosity-dependence of elastic moduli and hardness of 3Y-TZP ceramics, Ceram. Int. 25 (3) (1999) 281–286.
[19] M. Barsoum, Fundamentals of Ceramics, Series in Materials Science and Engineering, McGraw-Hill, New York, 1997.
[20] Y.S. Shin, Y.-W. Rhee, S.-J.L. Kang, Experimental evaluation of toughening mechanisms in alumina–zirconia composites, J. Am. Ceram. Soc. 82 (5) (1999) 1229–1232.